Manipulation and Dynamics at the Atomic Scale: A Dual Use of the Scanning Tunneling Microscopy

Patrici Molinàs-Mata,* Andrew J. Mayne, and Gérald Dujardin

Laboratoire de Photophysique Moléculaire, C.N.R.S., Université de Paris-Sud, Bât. 213, 91405 Orsay Cedex, France
(Received 10 February 1997)

Atomic scale modification of surfaces may trigger off dynamical processes. This is shown here by using the tip of a scanning tunneling microscope to extract an individual atom in a controlled manner from a predefined site of the reconstructed Ge(111)-$c(2\times8)$ surface. By thermally activated hopping of neighboring adatoms to the vacant site, the produced single-atom vacancy diffuses on the surface. From statistical analysis of the adatom configurations observed around the vacancy, we determine tiny (<0.15 eV) differences in free energy between the configurations. A linear increase of the configuration free energy with the number of adatoms located at metastable T_4 sites is reported. [S0031-9007(98)05608-7]

Matter can be manipulated atom by atom [1–7] with the scanning tunneling microscope (STM) [8]. However, modifying a surface structure at the atomic level does not necessarily result in a stable configuration at the temperature at which the modification has been performed. On the contrary, it may induce a dynamical process, whose evolution in time can be traced by imaging with the STM. Ideally, one could take advantage of the combined use of the STM as an atomic manipulator to create a desired arrangement of atoms and as an atomic viewer to monitor the dynamics which result. This could provide outstanding insights on the magnitudes of the physical properties of interest, like the differences in free energy between the different atomic configurations observed during the dynamical process.

Here we report such an experiment using the STM tip to extract an individual germanium (Ge) adatom from a predefined site of the top layer of the Ge(111)-$c(2\times8)$ reconstructed crystal surface [9,10]. The resulting single-atom vacancy (SAV) moves on the surface by thermally activated hopping of the neighboring atoms to the vacant site. The motion of the vacancy is sampled by recording a series of STM topographs of the surface. By analyzing statistically the STM snapshots of the SAV diffusion, we obtain the differences in free energy between the observed configurations. Note that adatom dynamics following the single-adatom extractions reported here may significantly differ from the dynamical processes which occur on the same surface when increasing the temperature [11] or after deposition of submonolayer amounts of lead [12] or indium [13].

Regular Ge(111)-$c(2\times8)$ surfaces, like the one shown in Fig. 1(a), are routinely prepared in UHV by Ar-sputtering ($E_{\text{beam}} = 500$ eV) while holding the surface at 640 °C using resistive heating [14]. In order to produce with the STM a SAV in the surface as in Fig. 1(b), we use a method somewhat similar to that used to extract atoms from silicon [3–5] and MoS$_2$ [6] surfaces. The

tip (an electrochemically etched polycrystalline tungsten wire) undergoes a sequence of four events to extract an atom. (1) The tip is positioned over the chosen adatom; as indicated by the arrow in Fig. 1(a). (2) The feedback loop is opened, and the tip approached towards the adatom ≈ 2 Å stepwise over 25 ms. (3) The sample-to-tip voltage, V_s, is increased from the topographic value of $+1$ to $+4$ V and kept constant during 10 ms. (4) V_s is reset to $+1$ V, and then, the tip is withdrawn from the surface over 25 ms stepwise as for the approach.

By this procedure, we can create SAV's in a reproducible way. However, the structure and chemistry of the apex of the tip or microtip [15] responsible for electron tunneling becomes a parameter of extreme importance in our experiment when quantifying the probability of producing a SAV for the same tip-approach length and voltage-pulse duration and magnitude. A precise determination of the extraction probabilities as a function of the various parameters will be presented elsewhere. We mention here, however, that all analyzed images were taken with microtips which display, for $V_s = 1$ V, a corrugation contrast between ad- and rest atoms larger than 1 Å as shown in Fig. 1. This corrugation is not typically obtained after *in situ* Ar$^+$ sputtering [16] or tip annealing by e^- bombardment, which produce, for the same V_s, topographs where both the ad- and rest atoms appear with comparable (<0.1 Å) corrugation. We switch from the latter conditions, achieved after tip annealing, to the huge corrugation differences between adatoms and rest atoms in Figs. 1 and 2 by performing the process mentioned above for atomic extraction. This indicates that the apex of the tip is likely to be ended by a Ge atom. Such microtips let us perform several extractions before changes in the corrugation or in the $I(z)$ curves are perceptible.

Naturally occurring defects, as the feature appearing at the top right corner of Figs. 1(a) and 1(b) do not move at room temperature and, thus, can be used, unmistakably, as reference points during the experiment
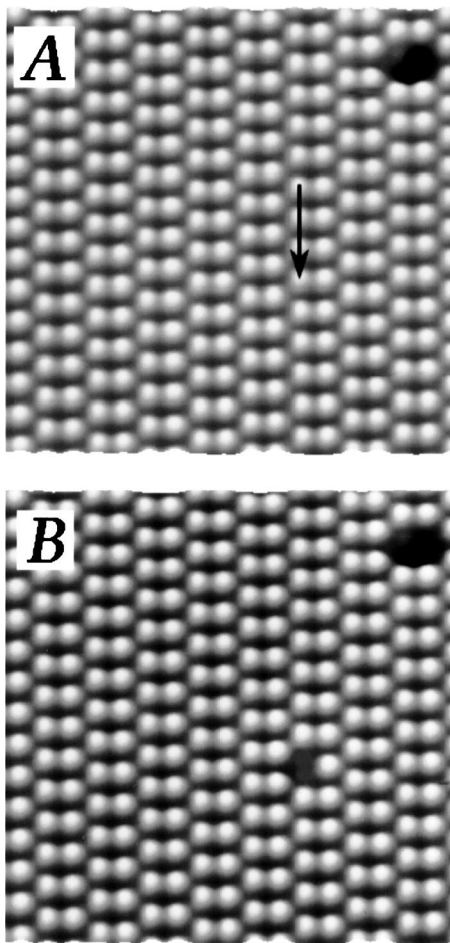
FIG. 1. A 115×115 Å^2 STM topograph of the Ge(111)-$c(2\times8)$ surface ($V_s = +1$ V and $I_t = 1$ nA). (a) The naturally occurring defect in the top right corner acts as a reference point. The arrow indicates the germanium atom on top of which the tip is positioned for atom extraction. (b) The result of the tip action showing the creation of a single-atom vacancy (SAV). Horizontal and vertical axes are parallel to the [$\overline{1}\overline{1}2$] and [$1\overline{1}0$] directions, respectively.

FIG. 2. STM topographic images of the same 55×70 Å^2 area of the Ge(111)-$c(2\times8)$ surface (with $+1$ V and 1 nA) which map out the diffusion of an STM-produced vacancy. While $t = 0$, 46, 94, 141, 187, 234, and 281 s are consecutive snapshots of the surface, $t = 797$ and 1036 s have been chosen among later topographs to show configurations with three and six adatoms at metastable T_4 sites, respectively.

because of their ≈ 0.5 Å lower corrugation. Vacancy displacement is monitored by scanning a $\sim 150\times150$ Å^2 large region, typically, at ~ 40 s/frame. Between two successive topographs, the net vacancy displacement is the result of a series of elementary adatom jumps which correspond to atom hopping from occupied to empty T_4 sites. The vacancy motion is not induced by the STM tip itself since the number of STM snapshots showing adatom motion during the scanning process is similar to the number expected given the time required to scan an adatom.

Figure 2 ($t = 0$, 46, 94, and 187 s) shows the most observed adatom arrangements for a vacancy; all the adatoms are sitting at the stable T_4 sites, i.e., the occupied positions in an intact Ge(111)-$c(2\times8)$ surface. The two nonequivalent configurations for these atomic arrangements are depicted in Figs. 3(a) and 3(b). Although less
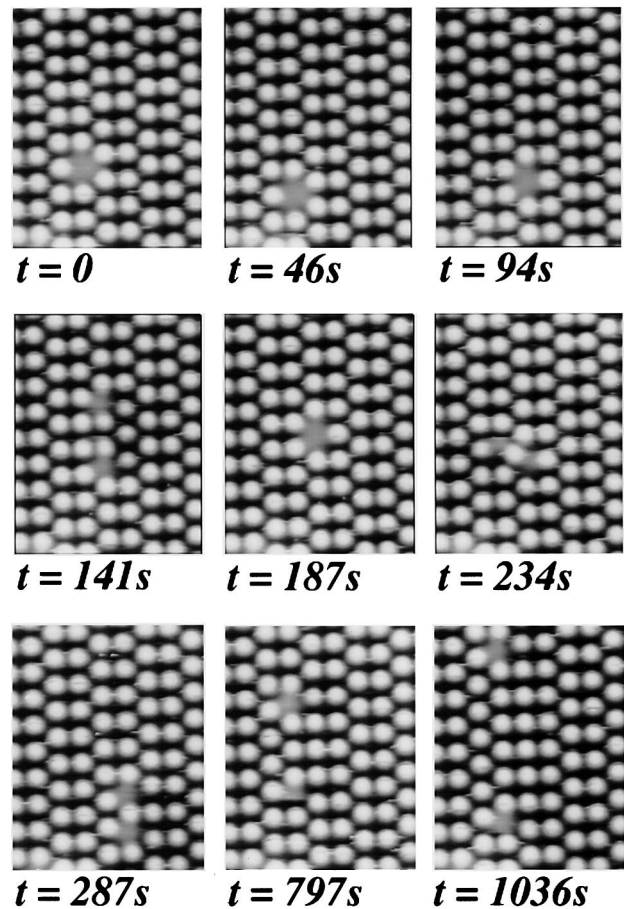
often, the adatoms also appear in the four [17] nonequivalent configurations c, d, e, and f displayed in Fig. 3 [see, for example, Fig. 2 ($t = 234$ and 287 s)]. There, one adatom stays at a metastable T_4 site, empty in the pristine Ge(111)-$c(2\times8)$. For these configurations the vacancy splits over two nearest-neighbor stable T_4 sites. If more than one single metastable T_4 site is occupied at the same time—as in Fig. 2 ($t = 141$, 797, and 1036 s)—the vacancy extends over more than two stable sites along the [$1\overline{1}0$] direction. The more adatoms there are at metastable T_4 sites, the less often we observe such a configuration. In fact, no configuration involving more than six adatoms as in Fig. 2 ($t = 1036$ s) has been seen, and only those up to 4 atoms shown in Figs. 3(g)–3(l) appear sufficiently often to be included in the data analysis. In agreement with calculations [10,18,19], we have never observed adatoms sitting at the very unstable H_3 sites; for example, at the site midway between the vacancy locations in Figs. 3(a) and 3(b). Note that we distinguished,
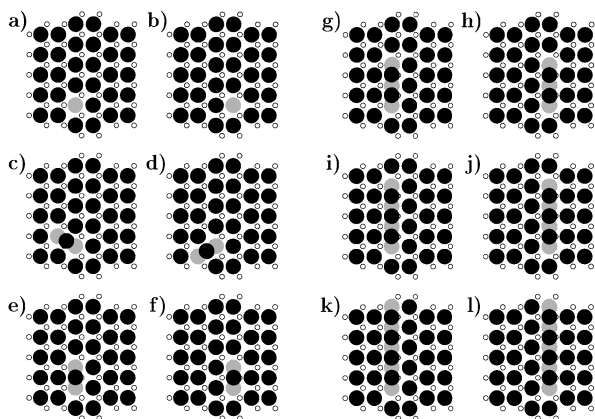
FIG. 3. Schematic representation of the nonequivalent adatom arrangements at an STM-produced vacancy. In (a) and (b) all the adatoms stay at stable T_4 sites, whereas for the remaining configurations, a single adatom [(c) to (f)] or several [(g) to (l)] occupy metastable T_4 sites. Filled circles correspond to the adatoms and smaller open ones to the unsaturated atoms at the second atom layer or rest atoms [9,10].

from one another, the configurations a and b, c and d, etc., by imaging at negative sample bias [14,16].

The motion of the STM-generated vacancies ends when the vacancy merges with a naturally produced island of vacancies, which increases its number of empty sites by one. Vacancies can also get trapped, probably by underlying substitutional atomic defects [14]. Diffusion series with extremely long mean times between consecutive vacancy displacements or where vacancies hardly move are not considered in this analysis. From four series of images recorded at ≈40 s/frame over elapsed times of 4237, 3000, 1399, and 738 s, we estimate the probabilities, p_α, (see Table I) of observing one of the 12 different configurations shown in Fig. 3. The probability of observing a local adatom distribution depends on the free energy for the occupied adatom sites. The lower the free energy of a configuration, the more frequently this configuration is observed. The fact that the two empty T_4 atomic sites (configurations a and b displayed in Fig. 3) are surrounded by 3 and 4 rest atoms, respectively, implies that an adatom at these two sites does not have exactly the same binding

TABLE I. Measured probabilities (in %) of observing one of the 12 adatom configurations in Fig. 3 during the diffusion of a single-adatom vacancy purposely created with the STM tip on the Ge(111)-$c(2\times8)$.

a	b	g	h
44.3 ± 4.1	28.8 ± 3.3	3.8 ± 1.2	0.86 ± 0.57
c	d	i	j
7.8 ± 1.7	3.3 ± 1.1	2.00 ± 0.88	0.77 ± 0.54
e	f	k	l
4.6 ± 1.3	2.5 ± 1.0	0.87 ± 0.57	(0.4 ± 0.4)

energy. This corresponds to the difference in electronic charge transferred from the adatom to the surrounding 3 or 4 rest atoms as has been shown by *ab initio* calculations [10]. Not surprisingly, the free energies for configurations a and b also differ since configuration a is about twice more probable than b (see Table I). Less frequently observed configurations correspond to distributions of adatoms at metastable T_4 sites (configurations c to l shown in Fig. 3), whose free energies must lie higher than those for configurations a and b.

It could be argued that there are some other configurations of comparable free energies which have not been observed because of the high activation-energy barriers separating them from the observed ones. Fortunately, the covalent nature of bonding in Ge reduces the possible locations for Ge adatoms to the T_4 and H_3 sites only. As mentioned, calculations have shown that H_3 sites are largely unfavored energetically. Therefore, the observed vacancies visit all the relevant configurations in phase space. Thus, the system can be reasonably assumed to be in thermodynamic equilibrium. With this assumption, we extract the differences in free energy (which includes the binding energy and the vibrational entropy contribution) between configurations. In Fig. 4 we display the free energy at 27 °C for each configuration as a function of its number of adatoms at metastable T_4 sites along atom rows, n. As expected, the free energy increases with n. Within the error bars, the increase is constant: 14 ± 5 meV per each new adatom at a metastable site. Furthermore, this slope is independent of the side of the unit cell where the vacancy is located. The extrapolation of the linear behavior of the free energy towards $n = 0$ does not coincide with the free energies of the nonsplit
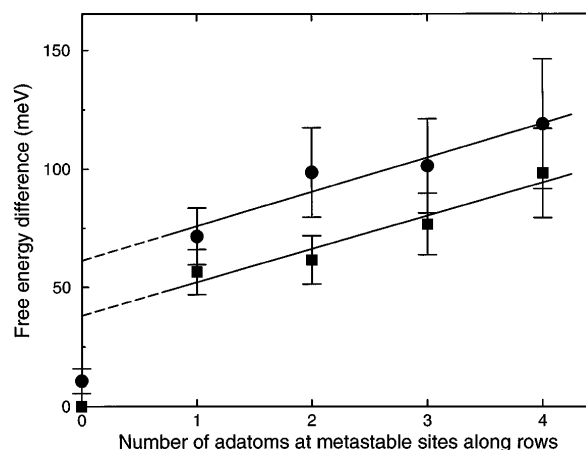

FIG. 4. Free energy for the adatom configurations observed at an STM-produced single-atom vacancy as a function of the number of adatoms located at metastable sites along [1$\bar{1}$0]. Assuming thermodynamical equilibrium we have converted the probabilities in Table I to free energies, for each configuration. Squares and circles correspond to the configurations a, e, g, i, k and b, f, h, j, l shown in Fig. 3, respectively.

vacancies (configurations a and b). Indeed, the difference between the extrapolated values and the actual free energies for $n = 0$ should be caused by the change of the vacancy boundaries when the vacancy splits in two. Consistently with our picture, when the number of adatoms at metastable sites, n, is larger than 1, the two boundaries of the two half-vacancies do not change significantly by varying n and, therefore, the configuration free energy is driven mainly by n.

In conclusion, studying the diffusion of a single-adatom vacancy produced with the STM tip on a Ge(111)-$c(2\times8)$ surface, has enabled us to obtain information in unprecedented detail on the energetics of Ge adatoms on that surface. Free energy differences between adatom configurations have been obtained and, therefore, this offers the possibility of a direct comparison with future theoretical calculations. Variable temperature measurements, however, are required to determine the contribution of the vibrational entropy to the reported differences in free energy. The method developed here on the Ge(111) surface is based on the combined use of the STM, as an atomic manipulator and an atomic scale viewer, to study single atom vacancy-motion. By pursuing at lower temperature the experiment reported in this Letter, it could be feasible to fabricate patterns made out of perfect rows of single adatom vacancies. Moreover, it should be checked if controlled adatom extraction followed by site-selective adsorbate deposition with the STM-tip could help with the realization of in-plane atomic scale devices on Ge(111)-$c(2 \times 8)$.

*Present address: SRMP, CEA-Saclay, Bât. 520, 91191 Gif sur Yvette, Cedex, France.
Electronic address: molinas@srmp11.saclay.cea.fr

[1] R. S. Becker et al., Nature (London) **325**, 419 (1987).
[2] D. M. Eigler et al., Nature (London) **344**, 524 (1990).
[3] I.-W. Lyo et al., Science **253**, 173 (1991).
[4] H. Uchida et al., Phys. Rev. Lett. **70**, 2040 (1993).
[5] C. T. Salling et al., Science **265**, 502 (1994).
[6] S. Hosaka et al., J. Vac. Sci. Technol. B **13**, 2813 (1995).
[7] G. Meyer et al., Phys. Rev. Lett. **77**, 2113 (1996).
[8] G. Binnig et al., Phys. Rev. Lett. **50**, 120 (1983).
[9] R. Feidenhans'l et al., Phys. Rev. B **38**, 9715 (1988).
[10] N. Takeuchi et al., Phys. Rev. Lett. **69**, 648 (1992); Phys. Rev. B **51**, 10 844 (1995).
[11] R. M. Feenstra et al., Phys. Rev. Lett. **66**, 3257 (1991).
[12] I.-S. Hwang et al., Science **258**, 1119 (1992); **265**, 490 (1994).
[13] Z. Gai et al., Phys. Rev. B **53**, 13 547 (1996).
[14] P. Molinàs-Mata et al., Phys. Rev. B **47**, 10 319 (1993).
[15] T. Klitsner et al., Phys. Rev. B **41**, 3837 (1990).
[16] P. Molinàs-Mata, Ph.D. thesis, University of Stuttgart, 1993.
[17] The configurations c and d shown in Fig. 3 are not equivalent because there is a small in-plane asymmetry between the two adatoms and rest atoms. This rules out the seeming mirror-plane symmetry perpendicular to the double rows of adatoms as discussed in [10] and in P. Molinàs-Mata et al., Mater. Res. Soc. Symp. Proc. **295**, 207 (1993).
[18] N. Takeuchi et al., Surf. Sci. **307**, 755 (1994).
[19] E. Kaxiras, Thin Solid Films **272**, 386 (1996), and references therein.